Competition and Interplay between σ-Hole and π-Hole Interactions: A Computational Study of 1:1 and 1:2 Complexes of Nitryl Halides (O 2 NX) with Ammonia

ARTICLE *in* THE JOURNAL OF PHYSICAL CHEMISTRY A · APRIL 2012

Impact Factor: 2.69 · DOI: 10.1021/jp300540z · Source: PubMed

6 AUTHORS, INCLUDING:

Mohammad Solimannejad
Arak University
167 PUBLICATIONS **1,589** CITATIONS
SEE PROFILE

Vahid Ramezani
Arak University
1 PUBLICATION **29** CITATIONS
SEE PROFILE

Cristina Trujillo
Trinity College Dublin
36 PUBLICATIONS **395** CITATIONS
SEE PROFILE

Goar Sánchez
University College Dublin
69 PUBLICATIONS **905** CITATIONS
SEE PROFILE

THE JOURNAL OF PHYSICAL CHEMISTRY A

Article

pubs.acs.org/JPCA

Competition and Interplay between σ-Hole and π-Hole Interactions: A Computational Study of 1:1 and 1:2 Complexes of Nitryl Halides (O_2NX) with Ammonia

Mohammad Solimannejad,*[,†] Vahid Ramezani,[†] Cristina Trujillo,[‡] Ibon Alkorta,*[,‡] Goar Sánchez-Sanz,[‡] and José Elguero[‡]

[†]Quantum Chemistry Group, Department of Chemistry, Faculty of Sciences, Arak University, Arak 38156-8-8349, Iran

[‡]Instituto de Química Médica (CSIC), Juan de la Cierva, 3, 28006 Madrid, Spain

Supporting Information

ABSTRACT: Quantum calculations at the MP2/cc-pVTZ, MP2/aug-cc-pVTZ, and CCSD(T)/cc-pVTZ levels have been used to examine 1:1 and 1:2 complexes between O_2NX (X = Cl, Br, and I) with NH_3. The interaction of the lone pair of the ammonia with the σ-hole and π-hole of O_2NX molecules have been considered. The 1:1 complexes can easily be differentiated using the stretching frequency of the N−X bond. Thus, those complexes with σ-hole interaction show a blue shift of the N−X bond stretching whereas a red shift is observed in the complexes along the π-hole. The SAPT-DFT methodology has been used to gain insight on the source of the interaction energy. In the 1:2 complexes, the cooperative and diminutive energetic effects have been analyzed using the many-body interaction energies. The nature of the interactions has been characterized with the atoms in molecules (AIM) and natural bond orbital (NBO) methodologies. Stabilization energies of 1:1 and 1:2 complexes including the variation of the zero point vibrational energy (ΔZPVE) are in the ranges 7−26 and 14−46 kJ mol^{-1}, respectively.

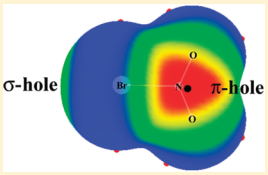

1. INTRODUCTION

Noncovalent interactions between molecules play an important role in supramolecular chemistry, molecular biology, and materials science.[1] Recently, interest in new types of intermolecular interactions, such as σ-hole and π-hole interactions, has grown. When a half-filled p orbital participates in the formation of a covalent bond, its electron normally tends to be localized in the internuclear region, thereby diminishing the electronic density in the outer (noninvolved) lobe of that orbital. This electron-deficient outer lobe of a half-filled p orbital involved in a covalent bond is called a "σ-hole".[2] Positive σ-holes have now been found computationally on the outer surfaces of group V, VI, and VII atoms in numerous molecules.[3−6] A positive π-hole is a region of positive electrostatic potential that is perpendicular to a portion of a molecular framework. It is the counterpart of a σ-hole, which is along the extension of a covalent bond to an atom.[7]

Great interest has been shown in recent years in the so-called reservoir compounds in the atmosphere and much effort has been devoted to an understanding of their molecular properties, isomerization processes and the role of the related formation reactions in stratospheric ozone depletion cycles.[8,9] Nitryl halides, XNO_2, have been suggested to be examples of such reservoir species.[10,11] Ammonia, as one of the most relevant molecules in nature, is important in many fields of science and technology. Despite the potential importance of nitryl halides and ammonia in atmospheric chemistry, to the best of our knowledge neither comprehensive and comparative theoretical study nor experimental investigations have been reported for complexes of NH_3 with O_2NX molecular moieties. In the absence of experimental information, a theoretical analysis of the possible existence of such complexes and their properties is in order. The present work thus focuses on a detailed study of the stabilities, electronic structure, and vibrational frequencies of 1:1 and 1:2 complexes formed between nitryl halides and ammonia via NH···N and N···N interactions. This work represents the first report of competition and interplay between σ-hole and π-hole interactions.

2. COMPUTATIONAL DETAILS

The structures of the monomers and the complexes were optimized and characterized by frequency computations at the MP2/cc-pVTZ computational level.[12,13] The def2-TZVPP (default-2 triple-ζ valence with the large polarization basis set) with pseudopotential have been used for iodine.[14] The contraction scheme of this basis set is [6s5p3d2f] for I atom. In a recent paper, Riley et al.[15] pointed out that this method provides very good estimates of the geometries and energies for noncovalent complexes. In addition, MP2/aug-cc-pVTZ and CCSD(T)/cc-pVTZ optimization has been carried out in the 1:1 complexes. Calculations were performed using the Gaussian03 and Gaussian09 programs.[16,17] The stabilization energy was calculated as the difference of the total energy of the complexes and the sum of the isolated monomers in their minima configurations. In addition, the interaction energy has been calculated using the energy of the monomers with the

Received: January 16, 2012
Revised: April 11, 2012
Published: April 16, 2012

geometry of the complex calculated with the full basis set. The difference between the stabilization energy and the interaction energy corresponds to the distortion of the monomers. In all cases, the reported energies correspond to that corrected from the inherent basis set superposition error (BSSE) using the full counterpoise (CP) method.[18]

The atoms in molecules (AIM) methodology[19,20] was used to analyze the electron density of the systems with the AIMAll program.[21] The natural bond orbital (NBO) method has been employed to evaluate atomic charges using the NBO-3 program, and to analyze charge-transfer interactions between occupied and unoccupied orbitals. The molecular electrostatic potential on the electron density isosurface of 0.001 a.u has been obtained and depicted using the WFA program.[22]

The SAPT (symmetry adapted perturbation theory)[23] method allows for the decomposition of the interaction energy into different terms related to physically well-defined components, such as those arising from electrostatic, exchange, induction, and dispersion terms. The interaction energy can be expressed within the framework of the SAPT method as

$$E_{int} = E_{el}^{(1)} + E_{exch}^{(1)} + E_{i}^{(2)} + E_{D}^{(2)} \quad (1)$$

where $E_{el}^{(1)}$ is the electrostatic interaction energy of the monomers each with its unperturbed electron distribution; $E_{exch}^{(1)}$ is the first-order exchange energy term; $E_{i}^{(2)}$ denotes the second-order induction energy arising from the interaction of permanent multipoles with induced multipole moments and charge-transfer contributions, plus the change in the repulsion energy induced by the deformation of the electronic clouds of the monomers; and $E_{D}^{(2)}$ is the second-order dispersion energy, which is related to the instantaneous multipole-induced multipole moment interactions plus the second-order correction for coupling between the exchange repulsion and the dispersion interactions.

The DFT-SAPT formulation has been used to investigate interaction energies. In this approach, the energies of interacting monomers are expressed in terms of orbital energies obtained from Kohn−Sham density functional theory.[24,25] In addition to the terms listed in eq 1, a Hartree−Fock correction term δ(HF), which considers higher-order induction and exchange corrections, has been included.[26] The DFT-SAPT calculations have been performed using the PBE0 funtional and the aug-cc-pVTZ basis set for all the atom except for the iodine one where the LANL2DZ basis set has been used.[27] The asymptotic corrections for this functional have been considered using the experimental values of the ionization potentials for NH_3, NO_2F, and NO_2Cl.[28,29] In the rest of the cases, the calculated values of the ionization potentials at the MP2/cc-pVTZ computational values have been used. All the calculations have been carried out with the MOLPRO program.[30] The DFT-SAPT energies have been shown to be of similar quality to those provided by CCSD(T) calculations.[31,32]

3. RESULTS

Monomers. The geometry in gas phase of three nitryl halides is known and has been compared to those obtained at MP2/cc-pVTZ computational level in Table 1. Both experiments and calculations show that the minima correspond to a C_{2v} symmetry geometry. The N−O bond distances are well reproduced by the computational method, whereas the calculated N−X ones are about 0.04 Å longer than the experimental ones. In the same way, the ONO angles provided by our ab initio calculations are about 2° longer than the experimental ones. In any case, the evolution of the distances, calculated or experimental are the same. Thus, the N−O bond distance increases as the X atom does whereas the ONO bond angle decreases as the atomic number of X increases.

Table 1. Calculated Results at the MP2/cc-pVTZ Computational Level of the Geometry of the Nitryl Halides (Å, deg)[a]

	N−O distance	N−X distance	ONO angle
NO_2F[b]	1.180 (1.1792)	1.493 (1.4560)	137.1 (135.49)
NO_2Cl[c]	1.192 (1.1916)	1.897 (1.8467)	133.7 (131.78)
NO_2Br[d]	1.195 (1.1956)	2.042 (2.0118)	132.9 (131.02)
NO_2I	1.202	2.197	131.0

[a]The available experimental parameters are shown in parentheses. [b]Experimental values from ref 33. [c]Experimental values from ref 34. [d]Experimental values from ref 35.

Among the electronic properties of these molecules, the molecular electrostatic potential (MEP) has been chosen to find those regions where electron rich moieties can interact with the NO_2X (Figure 1). The values of the MEP maxima on the 0.001 au electron density surface of the molecules show two positive regions, one above the nitrogen atom (π-hole) for the four molecules and another along the N−X bond (σ-hole), except in the case of NO_2F. The MEP values obtained in the σ- and π-hole at both MP2/cc-pVTZ and MP2/aug-cc-pVTZ levels are similar, being slightly more positive at the second computational level considered. In contrast, negative regions are found surrounding the oxygen atoms and perpendicular to the N−X bond. The values of the minima and maxima on the mentioned surface are gathered in Table 2.

1:1 Nitryl Halide−Ammonia Complexes. Two different configurations have been considered for the interaction of ammonia with the nitryl halides (Scheme 1). The first one corresponds to the interaction of the lone pair of ammonia with the σ-hole of the halide of NO_2X (configuration I). In the second one, the interaction is between the lone pair of ammonia with the π-hole of the nitryl halide (configuration II).

The stabilization, E_s, and interaction energies, E_i, of the complexes are reported in the first and second column of Table 3, and the values including the variation of the zero-point vibration energy, ΔZPVE, are given in the third column. The interaction energies, obtained with the cc-pVTZ and aug-cc-pVTZ, are almost identical. However, the effect of the BSSE is larger with the smaller basis set than with the larger one. Because the interaction energy at the extrapolated complete basis set (CBS) limit should be between the values obtained for the uncorrected and corrected ones,[36] it is clear that the BSSE correction at the MP2/cc-pVTZ level is overestimated. The CCSD(T) method provides stabilization and interaction energies that are within the range defined by the two MP2 calculations considered here for the complexes in configuration I and smaller in absolute values than the MP2 values for the complexes in configuration II. With respect to the interatomic distances, the CCSD(T) method provides slighlty larger interatomic distances than the ones obtained by the MP2 methods.

No complex in configuration I has been found between NO_2F and NH_3, because the NO_2F molecule shows the negative value of the σ-hole region where the interaction happens whereas in the rest of the nitryl derivatives it is positive. The interaction energies of the complexes between the

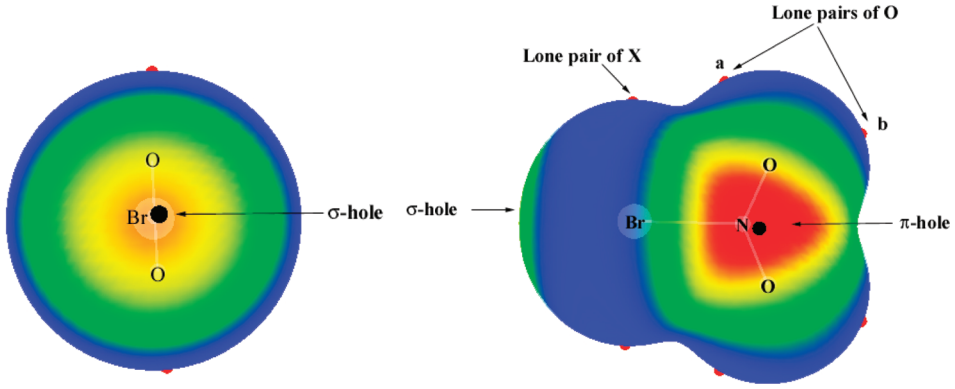

Figure 1. Two view of the molecular electrostatic potential on the 0.001au surface for $BrNO_2$. MEP values color scheme: red, >0.0309; yellow, >0.0170; green, >0.0031; blue, <0.0031.

Table 2. Maximum and Minimum Values of the MEP on the 0.001 au Electron Density Surface Calculated at the MP2/cc-pVTZ Computational Level (MP2/aug-cc-pVTZ in Parentheses)[a]

	σ-hole	π-hole	X lone pairs	oxygen atoms-a	oxygen atoms-b
NO_2F	−0.0141	0.0559	−0.0204	−0.0104	−0.0011
	(−0.0162)	(0.0590)	(−0.0229)		(0.0027)
NO_2Cl	0.0210	0.0475	−0.0106	−0.0105	−0.0047
	(0.0247)	(0.0490)	(−0.0085)	(−0.0154)	(−0.0062)
NO_2Br	0.0303	0.0448	−0.0089	−0.0108	−0.0062
	(0.0346)	(0.0454)	(−0.0062)	(−0.0110)	(−0.0092)
NO_2I	0.0469	0.0375	−0.0043	−0.0141	−0.0138
	(0.0494)	(0.0386)	(−0.0025)	(−0.0134)	(−0.0154)

[a]Oxygen atoms present two minima a and b, which corresponds to the minimum closer and further to the X atom, respectively.

Scheme 1. Two Configurations Considered for the 1:1 Amonia−Nitryl Halide Complexes

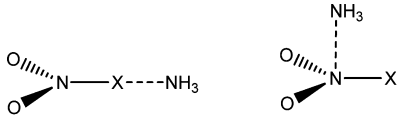

ammonia and the halogen atoms of the NO_2X molecules increase with the size of the halogen atom.

In the case of the complexes between the ammonia and the π-hole (configuration II), the opposite tendency is observed and the largest interaction energy is obtained for the fluoro derivative and the smallest for the iodine one, in agreement with the values of the MEP observed in the interaction region. Actually, linear correlations can be obtained between the values of the MEP (Table 2) and the interaction energies (Table 3) in the two series of complexes (Figure 2). The fact that the electron acceptor moieties in the two configurations are different, halogen atoms in configuration I and nitrogen in configuration II, does not allow us to obtain a single correlations for all of them.

The intermolecular distances found in the σ-hole interaction complexes (configuration I) are between 2.69 and 2.78 Å at MP2/cc-pVTZ level and between 2.63 and 2.76 Å at MP2/aug-cc-pVTZ level. The shortest distance is found in the complex with NO_2Br whereas the largest one is with the NO_2Cl at both computational levels.

The N···N distances in the π-hole interaction complexes (configuration II) increases with the size of the halogen atom present in the NO_2X molecules, in concordance of the tendency of the interaction energies obtained. In any case, the intermolecular distances obtained are larger than those found in the complexes in configuration I even though the size of the nitrogen atom in NO_2X is smaller than those of the X atoms.

Among the geometrical effects observed in the monomers due to the complexes, it is worth noting that the N−X bond in the nitryl halides are shorter in the σ-hole complexes (configuration I) than when isolated whereas they are longer in the π-hole complexes (configuration II) than isolated. These geometrical variations are associated to the blue and red shift of the N−X stretching in the σ-hole and π-hole interaction complexes, respectively. Several previous reports have reported the existence of blue shift XB.[37−40]

The SAPT energies (Table 4) indicate that in all the complexes the most important attractive contribution is the electrostatic one, representing between 54 and 57% of the sum of the attractive terms. This term increases with the size of the halogen atom in the complexes in configuration I whereas it decreases in the complexes in configuration II. The sum of the first-order terms is positive in both the complexes in configuration I and configuration II but in the former the values are much larger than in the latter. Between the second-order terms, the induction increases in the complexes configuration I with the size of the halogen atom. In the case of the complexes configuration II, all the second-order terms show almost identical values independently of the halogenated derivative considered. The dispersion term in these complexes contributes around a 30% of all the attractive terms.

The topological analysis of the electron density shows the presence of a single intermolecular bond critical point (BCP) in

dx.doi.org/10.1021/jp300540z | J. Phys. Chem. A 2012, 116, 5199−5206

Table 3. Stabilization, E_s, and Interaction, E_i, Energies (kJ mol^{-1}), Intramolecular Bond Length Changes, and Shift of NX Vibrational Stretching Frequency of O_2NX (cm^{-1}) upon Complex Formation at the MP2/cc-pVTZ/def2-TZVPP Level, MP2/aug-cc-pVTZ/aug-cc-pVTZ-PP in Parentheses and CCSD(T)/cc-pVTZ in Brackets

complexes	E_s	E_i	E_s + ΔZPVE	R(X···N) (Å)	R(N···N) (Å)	Δr(N−X) (mÅ)	Δω(N−X) (cm^{-1})
$O_2NCl\cdots NH_3$	−11.68	−13.49	−7.42	2.784		−56	54
(conf I)	(−13.96)	(−15.45)		(2.759)			
	[−13.34]	[−14.26]		[2.805]			
$O_2NBr\cdots NH_3$	−19.28	−22.04	−13.96	2.689		−58	48
(conf I)	(−23.34)	(−25.77)		(2.634)			
	[−20.96]	[−22.54]		[2.727]			
$O_2NI\cdots NH_3$	−32.22	−35.51	−25.74	2.699		−48	47
(conf I)	(−39.27)	(−41.77)		(2.655)			
$H_3N\cdots NO_2F$	−15.84	−16.42	−11.42		2.834	29	−26
(conf II)	(−18.94)	(−19.44)			(2.823)		
	[−14.01]	[−14.16]			[2.867]		
$H_3N\cdots NO_2Cl$	−14.38	−15.05	−10.07		2.881	43	−19
(conf II)	(−16.12)	(−16.72)			(2.899)		
	[−11.92]	[−12.04]			[2.937]		
$H_3N\cdots NO_2Br$	−13.83	−14.44	−9.76		2.904	40	−7
(conf II)	(−15.04)	(−15.59)			(2.916)		
	[−11.32]	[−11.42]			[2.956]		
$H_3N\cdots NO_2I$	−11.74	−12.02	−8.05		2.941	24	−2
(conf II)	(−13.13)	(−13.34)			(2.983)		

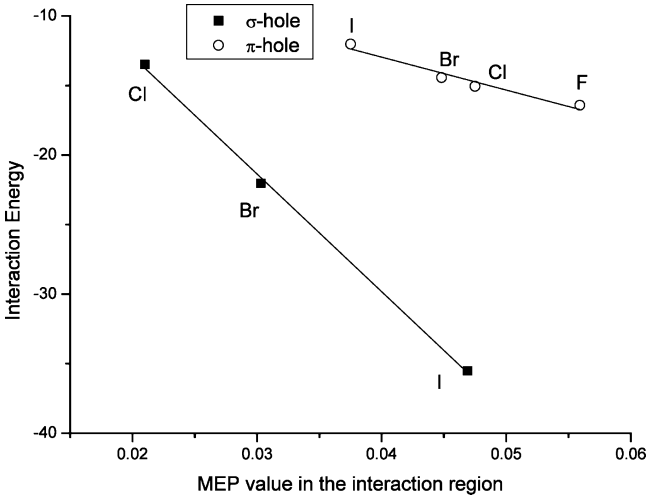

Figure 2. Interaction energy (kJ mol^{-1}) vs the MEP value (au) in the interaction region at the MP2/cc-pVTZ computational level. The linear correlation shows a square correlation coefficient of 0.94 and 0.99 for the σ-hole and π-hole values, respectively.

all the studied complexes. In the complexes in configuration I, the BCP corresponds to the linkage of the halogen atom of the NO_2X molecule with the nitrogen atom of NH_3, and in the complexes in configuration II, it bonds the two nitrogen atoms. The small values of the electron density and the small and positive values of the Laplacian in the intermolecular BCP correspond to closed shell interactions, similar to those found in other weak interactions.[41] In particular, it is interesting to notice that the values of the density and Laplacian at the BCP in the complexes in configuration I are larger than those found in configuration II.

The $-G_c/V_c$ ratio, G_c and V_c being respectively the kinetic and potential energy density at BCP, has been used as a measure of the covalency in noncovalent interactions. Values greater than 1 generally indicate a noncovalent interaction without covalent character whereas ratios smaller than unity are indicative of the covalent nature of the interaction.[42] The values for this quantity in Table 5 are around 1.27 in the complexes in configuration II whereas in the ones in configuration I this parameter decreases as the interaction becomes stronger. Thus, for the $O_2NI\cdots NH_3$ (configuration I) complex the value obtained is 0.92, an indication that the interaction starts to have a covalent nature.

The most important intermolecular second-order NBO charge-transfer energies, $E^{(2)}$, between full and empty orbital are reported in Table 5. The complexes in configuration I present an orbital interaction between the ammonia lone pair and the NX σ^* antibonding orbital in O_2NX whereas in the complexes in configuration II a charge transfer occurs between

Table 4. SAPT-DFT Energy Decomposition (kJ mol^{-1}), for All the Complexes at the MP2/aug-cc-pVTZ/LANL2DZ Level of Theory

complex	$E_{el}^{(1)}$	$E_{ex}^{(1)}$	$E_i^{(2)}$	$E_D^{(2)}$	δ(HF)	$\Delta E^{DFT\text{-}SAPT}$
$O_2NCl\cdots NH_3$ (conf I)	−36.8	53.1	−6.2	−15.2	−10.0	−15.1
$O_2NBr\cdots NH_3$ (conf I)	−70.4	99.0	−17.2	−22.5	−16.6	−27.8
$O_2NI\cdots NH_3$ (conf I)	−100.7	155.7	−59.5	−22.7	−12.3	−39.5
$H_3N\cdots NO_2F$ (conf II)	−30.8	31.6	−2.7	−13.6	−1.1	−16.6
$H_3N\cdots NO_2Cl$ (conf II)	−28.0	31.5	−2.7	−14.5	−1.0	−14.7
$H_3N\cdots NO_2Br$ (conf II)	−27.1	31.9	−2.7	−14.8	−1.0	−13.7
$H_3N\cdots NO_2I$ (conf II)	−25.0	32.1	−3.3	−14.2	−1.1	−11.5

dx.doi.org/10.1021/jp300540z | J. Phys. Chem. A 2012, 116, 5199−5206

Table 5. Electron Density Properties of the Intermolecular Bond Critical Points (au) Computed at MP2/cc-pVTZ/def2-TZVPP Computational Level and NBO Second-Order Energies $E(2)$ (kJ mol^{-1}) and Total Charge of the NO_2X Molecule Calculated at the HF/cc-pVTZ/def2-TZVPP Computational Level

	NX···N				
	ρ	$\nabla^2\rho$	$-G_c/V_c$	Q (me)	$E^{(2)}$ N(lp) → σ^*(NX)
O_2NCl···NH_3 (conf I)	0.0206	0.0708	1.12	−25	36.5
O_2NBr···NH_3 (conf I)	0.0292	0.0851	0.99	−52	78.1
O_2NI···NH_3 (conf I)	0.0342	0.0878	0.92	−75	118.6
	N···N				
	ρ	$\nabla^2\rho$	$-G_c/V_c$	Q (me)	$E^{(2)}$ N(lp) → σ^*(NO/NX)
H_3N···NO_2F (conf II)	0.0117	0.0508	1.27	−1.5	4.3
H_3N···NO_2Cl (conf II)	0.0111	0.0467	1.27	−0.6	4.2
H_3N···NO_2Br (conf II)	0.0108	0.0447	1.28	−0.5	4.1
H_3N···NO_2I (conf II)	0.0103	0.0421	1.28	−0.4	3.8/0.6

the lone pair of ammonia and the NX and NO σ^* antibonding orbital of O_2NX. The energy values of the orbital interactions found in the complexes in configuration I range between 36.5 kJ mol^{-1} for the NO_2Cl–NH_3 complex and 118.6 kJ mol^{-1} in the NO_2I–NH_3 one. In contrast, the values obtained for the complexes in configuration II range between 4.3 and 3.8 kJ mol^{-1} decreasing with the size of the halogen atom. The small values obtained for the complexes in configuration II are due to a small overlap of the two orbitals involved in the interaction which reduces the charge-transfer efficiency.

The analysis of the intramolecular orbital interactions in the O_2NX molecule shows that an important reduction is observed in the interaction between the lone pair of the oxygen atom and the σ^* of the N–X bond in the complexes in configuration I vs the one observed in the isolated molecules (Table 6). In

Table 6. Intramolecular NBO Second-Order Energies $E^{(2)}$ (kJ mol^{-1}) of the Interaction of the Oxygen Lone Pair Interaction with the σ^* of the N–X Bond

	isolated	conf I	conf II
FNO_2	329.2		366.7
$ClNO_2$	254.6	187.5	297.1
$BrNO_2$	234.1	153.1	272.9
INO_2	173.8	99.8	194.5

contrast, the same orbital interaction is larger in the complexes in configuration II than in the isolated molecules. The reduced $E^{(2)}$ for Conf I is consistent with a correspondingly lowered amount of charge transfer into the N–X antibond, which would result in a strengthening and shortening of the N–X bond.

1:2 Nitryl Halide–Ammonia Complexes. Three different dispositions of 1:2 nitryl halide–ammonia complexes have been considered (Scheme 2). Configuration III corresponds to the interaction of one ammonia molecule through the σ-hole and another through the π-hole. In the other two configurations (IV and V), one of the ammonia molecules interacts with one of the mentioned holes and the other molecule forms a bridging HB between the first ammonia molecule and the halogen atom of the NO_2X molecule. Due to the similar results obtained between the cc-pVTZ and aug-cc-pVTZ basis set in the 1:1 complexes, only the first one has been considered for the 1:2 complexes.

Scheme 2. Three Configurations of the 1:2 Nitryl Halide–Ammonia Complexes Considered

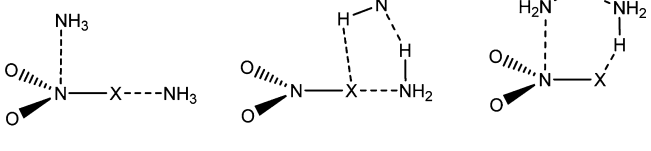

Conf. III Conf. IV Conf. V

The stabilization energies obtained in the 1:2 complexes (Table 7) range between −21 and −59 kJ mol^{-1} whereas the interaction energies range between −21 and −66 kJ mol^{-1}. The stabilization and interaction energies in configurations III and IV increase with the size of the halogen atom whereas in configuration V the opposite happens. In what concerns the intermolecular distances, a comparison with those reported with the analogous 1:1 complexes in Table 3 shows that the distances are longer in configuration III being shorter in configurations IV and V than in the 1:1 complexes.

With respect to the N–X bond stretching, the complexes that present σ-hole interactions (configurations III and IV) show a shortening of the N–X bond whereas in the complexes in configuration V a lengthening of the N–X is observed. Associated with these geometrical modifications, a blue shift is observed in configurations III and IV whereas a red shift is observed in configuration V. Using the data of the 1:1 and 1:2 complexes, linear relationships can be obtained between the N–X bond length and the bond stretching when the data are grouped on the basis of the X atom.

The nonadditive term of the interaction energy or cooperativity has been evaluated using the many-body interaction analysis.[43,44] For this purpose, the two and three-body contributions to total binding energy have been calculated. The two-body terms (ΔE_{A-B}, ΔE_{A-C}, and ΔE_{B-C}) correspond to the binding energy of each molecular pair in the geometry of triad minus the energy sum of the monomers, all of them frozen in the geometry of the triad. The three-body term ΔE_{A-B-C} is calculated as the total binding energy of the triad minus the interaction energy of each pair of monomers, all of them frozen in the geometry of the triad, using eq 2.[45]

$$\Delta E_{A-B-C} = E_i(ABC)' - \Delta E_{A-B} - \Delta E_{A-C} - \Delta E_{B-C} \quad (2)$$

The total relaxation energy (E_R) is defined as the energy sum of the monomers, all of then frozen in the geometry of the triads, minus the energy sum of the optimized monomers.

dx.doi.org/10.1021/jp300540z | J. Phys. Chem. A 2012, 116, 5199–5206

Table 7. Stabilization, E_s, and Interaction, E_i, Energies (kJ mol^{-1}), Intramolecular Bond Length Changes, and Shift of NX Vibrational Stretching Frequency of O_2NX (cm^{-1}) in the 1:2 Complexes at the MP2/cc-pVTZ/def2-TZVPP Computational Level

complexes	E_s	E_i	E_s + ΔZPVE	R(N−X···N) (Å)	R(N···N) (Å)	Δr(N−X) (mÅ)	Δω(N−X) (cm^{-1})
			Conformation III				
$H_3N{\cdots}NO_2Cl{\cdots}NH_3$	−20.50	−21.18	−13.91	2.905	2.940	−34	33
$H_3N{\cdots}NO_2Br{\cdots}NH_3$	−26.67	−30.31	−17.57	2.690	2.997	−73	61
$H_3N{\cdots}NO_2I{\cdots}NH_3$	−41.15	−45.73	−30.77	2.679	3.006	−62	57
			Conformation IV				
$H_3N{\cdots}NO_2Cl{\cdots}NH_3$	−29.72	−32.87	−17.87	2.635		−60	51
$H_3N{\cdots}NO_2Br{\cdots}NH_3$	−41.43	−46.89	−28.19	2.545		−46	46
$H_3N{\cdots}NO_2I{\cdots}NH_3$	−59.77	−66.10	−45.52	2.571		−41	47
			Conformation V				
$H_3N{\cdots}NO_2F{\cdots}NH_3$	−34.99	−37.26	−22.91		2.815	58	−39
$H_3N{\cdots}NO_2Cl{\cdots}NH_3$	−32.75	−34.75	−21.46		2.854	73	−50
$H_3N{\cdots}NO_2Br{\cdots}NH_3$	−31.89	−33.69	−20.84		2.868	79	−27
$H_3N{\cdots}NO_2I{\cdots}NH_3$	−24.43	−30.75	−14.10		2.906	33	−14

Table 8. Many-Body Interaction Analysis Energies (kJ mol^{-1})[a]

complex	conf	ΔE_{A-B}	ΔE_{A-C}	ΔE_{B-C}	E_R	ΔE_{A-B-C}
$H_3N{\cdots}NO_2Cl{\cdots}NH_3$	III	−18.31	−14.94	0.68	0.67	3.07
$H_3N{\cdots}NO_2Br{\cdots}NH_3$	III	−15.16	−29.62	1.51	3.63	0.12
$H_3N{\cdots}NO_2I{\cdots}NH_3$	III	−14.80	−46.89	1.22	4.58	−2.19
$H_3N{\cdots}NO_2Cl{\cdots}NH_3$	IV	−16.11	−4.94	−16.01	3.15	−6.60
$H_3N{\cdots}NO_2Br{\cdots}NH_3$	IV	−28.53	−6.14	−15.33	5.46	−11.92
$H_3N{\cdots}NO_2I{\cdots}NH_3$	IV	−45.81	−9.01	−14.55	6.32	−15.53
$H_3N{\cdots}NO_2F{\cdots}NH_3$	V	−22.12	−10.60	−15.96	2.27	−3.09
$H_3N{\cdots}NO_2Cl{\cdots}NH_3$	V	−20.65	−8.11	−15.77	2.00	−2.56
$H_3N{\cdots}NO_2Br{\cdots}NH_3$	V	−20.43	−8.15	−15.76	1.80	−2.43
$H_3N{\cdots}NO_2I{\cdots}NH_3$	V	−18.18	−7.90	−15.90	0.75	−1.99

[a]In all the cases the molecule A is the NO_2X derivative.

Table 9. Charge (me) of the NO_2X Molecule and NBO Second-Order Energies $E^{(2)}$ (kJ mol^{-1}) Calculated at the HF/cc-pVTZ/def2-TZVPP Computational Level

			$E^{(2)}$	
complexes	conf	Q of NO_2X	NX···N N(lp) → σ^*(NX)	N···N N(lp) → σ^*(NO/NX)
$H_3N{\cdots}NO_2Cl{\cdots}NH_3$	III	17	23.8	3.4
$H_3N{\cdots}NO_2Br{\cdots}NH_3$	III	49	76.3	1.3
$H_3N{\cdots}NO_2I{\cdots}NH_3$	III	78	124.0	1.3/0.3
$H_3N{\cdots}NO_2Cl{\cdots}NH_3$	IV	−45	61.8	
$H_3N{\cdots}NO_2Br{\cdots}NH_3$	IV	−92	136.2	
$H_3N{\cdots}NO_2I{\cdots}NH_3$	IV	−117	184.0	
$H_3N{\cdots}NO_2F{\cdots}NH_3$	V	0.6		4.6
$H_3N{\cdots}NO_2Cl{\cdots}NH_3$	V	0.6		4.3
$H_3N{\cdots}NO_2Br{\cdots}NH_3$	V	0.8		4.4
$H_3N{\cdots}NO_2I{\cdots}NH_3$	V	0.1		4.5

Thus, the total binding energy of the triad is obtained using eq 3.[45]

$$E_i(\mathrm{ABC}) = \Delta E_{A-B} + \Delta E_{A-C} + \Delta E_{B-C} + \Delta E_{A-B-C} + E_R \quad (3)$$

The results are presented in Table 8. All the second-order terms are attractive except the ammonia−ammonia term (ΔE_{B-C}) in the complexes in configuration III where these two molecules are not interacting among them. In those cases where a HB interaction exists between the NO_2X molecule and one of the ammonia molecules (configurations IV and V) it is represented by the ΔE_{A-C}. This term increases in the complexes in configuration IV with the size of the X atom whereas the opposite happens in the complexes in configuration V. The third-order term indicates diminutive effect for chlorine complex in configuration III whereas the bromine is neutral and the iodine one is slightly cooperative. In the case of the complexes in configuration IV, all are cooperative, increasing the cooperativity with the size of the halogen atom. Finally, small values of cooperativity are found in the complexes in configuration V, decreasing as the size of the halogen atom increases.

The NBO analysis of the 2:1 complexes (Table 9) shows that the orbital interaction in the complexes in configuration III are smaller than the corresponding ones in the 1:1 ones, except for the N(lp) → σ^*(NX) in the $NO_2I{-}(NH_3)_2$ (configuration III)

dx.doi.org/10.1021/jp300540z | J. Phys. Chem. A 2012, 116, 5199−5206

Table 10. AIM Properties (au) of Some of the Intermolecular Critical Points Computed at the MP2/cc-pVTZ/def2-TZVPP Level

		NX···N			N···N		
complexes	conf	ρ	$\nabla^2\rho$	$-G_c/V_c$	ρ	$\nabla\rho$	$-G_c/V_c$
$H_3N\cdots NO_2Cl\cdots NH_3$	III	0.0162	0.0563	1.1728	0.0099	0.0414	1.2984
$H_3N\cdots NO_2Br\cdots NH_3$	III	0.0290	0.0851	0.9962	0.0081	0.0394	1.3842
$H_3N\cdots NO_2I\cdots NH_3$	III	0.0353	0.0900	0.9085	0.0071	0.0371	1.4420
$H_3N\cdots NO_2Cl\cdots NH_3$	IV	0.0283	0.0906	1.0343			
$H_3N\cdots NO_2Br\cdots NH_3$	IV	0.0407	0.1024	0.8960			
$H_3N\cdots NO_2I\cdots NH_3$	IV	0.0445	0.0981	0.8319			
$H_3N\cdots NO_2F\cdots NH_3$	V				0.0128	0.0537	1.2364
$H_3N\cdots NO_2Cl\cdots NH_3$	V				0.0121	0.0501	1.2452
$H_3N\cdots NO_2Br\cdots NH_3$	V				0.0119	0.0491	1.2492
$H_3N\cdots NO_2I\cdots NH_3$	V				0.0111	0.0449	1.2664

that is slightly larger than the one observed in the NO_2I-NH_3 (configuration I) complex. The values obtained for the complexes in configurations IV and V are always larger than those found in the analogous 1:1 complexes, the differences being larger in the case of the complexes in configuration IV than those in configuration V. The charge observed for the NO_2X molecules are negative for those cases where X···N interactions are present whereas it is neutral when only N···N interactions are present, in accordance with the values of the orbital interactions observed.

The topological analysis of the electron density shows the presence of a variety of interactions in the 2:1 complexes: N···X, N···N, H···N, H···X, and X···O. The molecular graphs of these complexes are given in the Supporting Information. The values of the electron density and the Laplacian at the intermolecular N···X and N···N BCPs (Table 10) are smaller in the complexes in configuration III than those obtained of the corresponding 1:1 complexes whereas in configurations IV and V they are larger. These results are in agreement with the relationships found between the electron density and the interatomic distances in other weak interactions.[46,47] The variation of the values of the $-G_c/V_c$ parameter with respect to the analogous 1:1 complexes indicate a larger covalent character of the N···X and N···N interaction in the complexes in configurations IV and V, whereas in configuration III, the X···N are more covalent and the N···N less.

4. CONCLUSIONS

The equilibrium structures, vibrational frequencies, and cooperative effects on the properties of the 1:1 and 1:2 nitryl halide−ammonia complexes have been studied. Two configurations have been considered for the 1:1 complexes where the ammonia acts as an electron donor toward the σ-hole of the halogen atom of the nitryl halide (configuration I) and toward the π-hole of the nitrogen of NO_2X molecule (configuration II). The complexes via σ-hole interaction are more strongly bonded than those via π-hole interaction (the exceptions are the O_2NCl complexes). These results can be explained using the NBO and AIM analysis. The complexation is associated to a red shift or blue shift of the N−X bond stretching frequency of the NO_2X molecule as it engages respectively in N−X···N and N···N interactions in the 1:1 complexes. The magnitude of red shift ranges between 48 and 58 cm^{-1} for the 1:1 complexes and lies between 34 and 73 cm^{-1} for the 1:2 complexes. The N−X stretching frequency is shifted to the blue between 24 and 43 cm^{-1}.

The SAPT-DFT energy decomposition shows that the most contributing term to the total attractive forces is the $E_{el}^{(1)}$, which accounts for about 55% of the total. The different terms of the interaction energy are quite sensible to the halogen atom for the σ-hole interaction; meanwhile these terms remain almost invariant in the π-hole complexes.

Three configurations have been explored for the 2:1 complexes. Diminutive effects are observed in some of the complexes that show simultaneous interactions through σ- and π-holes (configuration III). In contrast, those complexes with a single ammonia molecule interaction with the σ- or π-hole whereas the other ammonia molecule bridges the first NH_3 with the halogen atom through HB interactions (configurations IV and V). The intermolecular distances found in the 2:1 complexes are in agreement with the energetic analysis previously described. Thus longer distances are found for complexes in configuration III whereas shorter distances are measured for those in configurations IV and V that the ones in the corresponding configurations I and II.

Blue shifts in the N−X bond stretching are observed in configurations III and IV whereas a red shift is observed in configuration V. Linear correlations are observed between the variation of the bond length and the variation of the bond stretching.

These findings should be helpful for understanding the cooperative and competitive role of σ-hole and π-hole bonding in molecular recognition, crystal engineering, and biological systems.

■ ASSOCIATED CONTENT

Ⓢ Supporting Information

Molecular graphs of the complexes studied. This material is available free of charge via the Internet at http://pubs.acs.org.

■ AUTHOR INFORMATION

Corresponding Author

*E-mail: M.S., m-solimannejad@araku.ac.ir; I.A., ibon@iqm.csic.es.

Notes

The authors declare no competing financial interest.

■ ACKNOWLEDGMENTS

We thank the Ministerio de Ciencia e Innovación of Spain (Project No. CTQ2009-13129-C02-02) and the Comunidad Autónoma de Madrid (Project MADRISOLAR2, ref S2009/PPQ-1533) for continuing support. Thanks are given to the

CTI (CSIC) and Centro de Computación Científica at Universidad Autónoma de Madrid for an allocation of computer time.

REFERENCES

(1) Müller-Dethlefs, K.; Hobza, P. *Chem. Rev.* **1999**, *100*, 143−168.
(2) Clark, T.; Hennemann, M.; Murray, J.; Politzer, P. *J. Mol. Model.* **2007**, *13*, 291−296.
(3) Auffinger, P.; Hays, F. A.; Westhof, E.; Ho, P. S. *Proc. Natl. Acad. Sci. U. S. A.* **2004**, *101*, 16789−16794.
(4) Politzer, P.; Lane, P.; Concha, M.; Ma, Y.; Murray, J. *J. Mol. Model.* **2007**, *13*, 305−311.
(5) Murray, J. S.; Lane, P.; Politzer, P. *Int. J. Quantum Chem.* **2007**, *107*, 2286−2292.
(6) Murray, J.; Concha, M.; Lane, P.; Hobza, P.; Politzer, P. *J. Mol. Model.* **2008**, *14*, 699−704.
(7) Murray, J.; Lane, P.; Clark, T.; Riley, K.; Politzer, P. *J. Mol. Model.* 1−8.
(8) Molina, M. J.; Rowland, F. S. *Nature* **1974**, *249*, 810−812.
(9) Wayne, R. P., *Chemistry of Atmospheres*; Oxford University Press: Oxford, U.K., 1991.
(10) Fickert, S.; Helleis, F.; Adams, J. W.; Moortgat, G. K.; Crowley, J. N. *J. Phys. Chem. A* **1998**, *102*, 10689−10696.
(11) Lesclaux, R.; Caralp, F.; Dognon, A. M.; Cariolle, D. *Geophys. Res. Lett.* **1986**, *13*, 933−936.
(12) Møller, C.; Plesset, M. S. *Phys. Rev.* **1934**, *46*, 618−622.
(13) Dunning, T. H. *J. Chem. Phys.* **1989**, *90*, 1007−1023.
(14) Weigend, F.; Ahlrichs, R. *Phys. Chem. Chem. Phys.* **2005**, *7*, 3297−3305.
(15) Riley, K. E.; Pitoňák, M.; Černý, J.; Hobza, P. *J. Chem. Theory Comput.* **2009**, *6*, 66−80.
(16) Frisch, M. J.; Trucks, G. W.; Schlegel, H. B.; Scuseria, G. E.; Robb, M. A.; Cheeseman, J. R.; Montgomery, J., J. A.; Vreven, T.; Kudin, K. N.; Burant, J. C., et al. *Gaussian-03*; Gaussian, Inc.: Wallingford, CT, 2003.
(17) Frisch, M. J.; Trucks, G. W.; Schlegel, H. B.; Scuseria, G. E.; Robb, M. A.; Cheeseman, J. R.; Scalmani, G.; Barone, V.; Mennucci, B.; Petersson, G. A., et al. *Gaussian 09*; Gaussian, Inc.: Wallingford, CT, 2009.
(18) Boys, S. F.; Bernardi, F. *Mol. Phys.* **1970**, *19*, 553−566.
(19) Bader, R. F. W. *Atoms in Molecules: A Quantum Theory*; Clarendon Press: Oxford, U.K., 1990.
(20) Popelier, P. L. A. *Atoms In Molecules. An introduction*; Prentice Hall: Harlow, England, 2000.
(21) Keith, T. A. *AIMAll*, version 11.10.16; TK Gristmill Software: Overland Park, KS, USA, 2011.
(22) Bulat, F.; Toro-Labbé, A.; Brinck, T.; Murray, J.; Politzer, P. *J. Mol. Model.* **2010**, *16*, 1679−1691.
(23) Jeziorski, B.; Moszynski, R.; Szalewicz, K. *Chem. Rev.* **1994**, *94*, 1887−1930.
(24) Misquitta, A. J.; Podeszwa, R.; Jeziorski, B.; Szalewicz, K. *J. Chem. Phys.* **2005**, *123*, 214103−14.
(25) Hesselmann, A.; Jansen, G. *Phys. Chem. Chem. Phys.* **2003**, *5*, 5010−5014.
(26) Moszynski, R. *Mol. Phys.* **1996**, *88*, 741−758.
(27) Perdew, J. P.; Burke, K.; Ernzerhof, M. *Phys. Rev. Lett.* **1997**, *78*, 1396−1396.
(28) Locht, R.; Hottmann, K.; Hagenow, G.; Denzer, W.; Baumgartel, H. *Chem. Phys. Lett.* **1992**, *190*, 124−129.
(29) Frost, D. C.; Lee, S. T.; McDowell, C. A.; Westwood, N. P. C *J. Electron Spectrosc. Relat. Phenom.* **1975**, *7*, 331−347.
(30) Werner, H.-J.; Knowles, P. J.; Manby, F. R.; Schütz, M.; Celani, P.; Knizia, G.; Korona, T.; Lindh, R.; Mitrushenkov, A.; Rauhut, G., et al. *MOLPRO, a package of ab initio programs*, version 2010.1; Molpro: Cardiff, U.K., 2010.
(31) Pitoňák, M.; Riley, K. E.; Neogrády, P.; Hobza, P. *ChemPhysChem* **2008**, *9*, 1636−1644.
(32) Karthikeyan, S.; Sedlak, R.; Hobza, P. *J. Phys. Chem. A* **2011**, *115*, 9422−9428.
(33) Demaison, J.; Császár, A. G.; Dehayem-Kamadjeu, A. *J. Phys. Chem. A* **2006**, *110*, 13609−13617.
(34) Francis, S. G.; Harvey, J. N.; Walker, N. R.; Legon, A. C. *J. Chem. Phys.* **2008**, *128*, 204305−10.
(35) Kwabia Tchana, F.; Orphal, J.; Kleiner, I.; Rudolph, H. D.; Willner, H.; Garcia, P.; Bouba, O.; Demaison, J.; Redlich, B. *Mol. Phys.* **2004**, *102*, 1509−1521.
(36) Alkorta, I.; Trujillo, C.; Elguero, J.; Solimannejad, M. *Comput. Theor. Chem.* **2011**, *967*, 147−151.
(37) Zou, W. S.; Han, J.; Jin, W. J. *J. Phys. Chem. A* **2009**, *113*, 10125−10132.
(38) Zhang, Y.; Li, A.-Y.; Cao, L.-J. *Struct. Chem.* **2012**, *23*, 627−636.
(39) Zhou, Z.-J.; Liu, H.-L.; Huang, X.-R.; Li, Q.-Z.; Sun, C.-C. *Mol. Phys.* **2010**, *108*, 2021−2026.
(40) Wang, W.; Zhang, Y.; Ji, B. *J. Phys. Chem. A* **2010**, *114*, 7257−7260.
(41) Rozas, I.; Alkorta, I.; Elguero, J. *J. Am. Chem. Soc.* **2000**, *122*, 11154−11161.
(42) Ziółkowski, M.; Grabowski, S. J.; Leszczynski, J. *J. Phys. Chem. A* **2006**, *110*, 6514−6521.
(43) Valiron, P.; Mayer, I. *Chem. Phys. Lett.* **1997**, *275*, 46−55.
(44) White, J. C.; Davidson, E. R. *J. Chem. Phys.* **1990**, *93*, 8029−8035.
(45) Hankins, D.; Moskowitz, J. W.; Stillinger, F. H. *J. Chem. Phys.* **1970**, *53*, 4544−4554.
(46) Alkorta, I.; Zborowski, K.; Elguero, J.; Solimannejad, M. *J. Phys. Chem. A* **2006**, *110*, 10279−10286.
(47) Mata, I.; Alkorta, I.; Molins, E.; Espinosa, E. *Chem.—Eur. J.* **2010**, *16*, 2442−2452.